ORNL/TM-2024/3403

Effect of Sample Thickness on the Tensile Strength of Small Graphite Discs

Lianshan Lin
Nidia C. Gallego

May 2024

OAK RIDGE National Laboratory

ORNL IS MANAGED BY UT-BATTELLE LLC FOR THE US DEPARTMENT OF ENERGY

ORNL/TM-2024/3403

Materials Science and Technology Division

EFFECT OF SAMPLE THICKNESS ON THE TENSILE STRENGTH OF SMALL GRAPHITE DISCS

Lianshan Lin
Nidia C. Gallego

May 2024

Prepared by
OAK RIDGE NATIONAL LABORATORY
Oak Ridge, TN 37831
managed by
UT-BATTELLE LLC
for the
US DEPARTMENT OF ENERGY
under contract DE-AC05-00OR22725

CONTENTS

LIST OF FIGURES

LIST OF TABLES

ABSTRACT

This report formally documents the completion of the Advanced Reactor Technologies (ART) Level 3 Milestone (M3TG-24OR0501054), "Continue activities related to Split Disc-DIC - complete analysis of effect of sample thickness on one fine grain graphite," due May 31, 2024. Details within this report outline the status of activities aimed at elucidating the effect of sample thickness on the tensile strength measurement using the small-disc, split-disc testing standard in support of the US Department of Energy's ART Graphite R&D Program.

The ASTM D8289, *Standard Test Method for Tensile Strength Estimate by Disc Compression of Manufactured Graphite*, was developed to provide an alternative means for testing tensile strength on smaller specimens, which are compatible with available irradiation capsule volumes, and other compatibility measurements. ASTM D8289 specifies that acceptable specimen diameter can range from 6 to 12.7 mm and that the maximum allowed sample thickness should be half of the diameter. However, information is limited with respect to the effect of thickness on the measured splitting tensile strength.

This report documents efforts to understand the effect of sample thickness on splitting tensile strength. The work involved testing Ø12.7 mm samples of fine-grain graphites 2114 and IG-110 of different thicknesses (6.35, 5, 4, and 3 mm). The digital image correlation (DIC) method was applied to the samples, along with the ASTM D8289 Standard, to help interpret the measured results.

1. INTRODUCTION

Graphite has been used as a neutron moderator and reflector in more than 100 nuclear power plants around the world and in many research and plutonium-production reactors as well. Because many important structural components in reactors are made of graphite, its mechanical properties such as tensile strength, fracture strength, Young's modulus, and fracture toughness before and after irradiation are crucial for the design of high-temperature reactors.

Unlike alloys, most nuclear graphites are porous, heterogeneous, and sometimes have anisotropic structure. These attributes make accurately measuring graphite's mechanical properties more difficult. Therefore, several test standards have been developed by ASTM to appropriately measure graphite's mechanical properties, such as three-point bending test ASTM D7972,[1] uniaxial tensile test ASTM C749,[2] ring-on-ring test ASTM C1499,[3] sonic test ASTM C769 to obtain elastic constants,[4] and fracture toughness test ASTM D7779.[5]

Among these tests, the uniaxial tensile test ASTM C749 is the most straightforward to obtain the elastic moduli, ultimate tensile strength, and the strain to failure for a wide range of graphites with grain sizes on the order of 1 mil to ¼ in. (0.0254–6.4 mm) and larger. However, the specimen size in general is large

[1] ASTM D7972-14(2020), Standard Test Method for Flexural Strength of Manufactured Carbon and Graphite Articles Using Three-Point Loading at Room Temperature, Annual Book of ASTM Standards, ASTM International, West Conshohocken, Pennsylvania, 2020.
[2] ASTM C749-15(2020), Standard Test Method for Tensile Stress-Strain of Carbon and Graphite, Annual Book of ASTM Standards, ASTM International, West Conshohocken, Pennsylvania, 2020.
[3] ASTM C1499-19, Standard Test Method for Monotonic Equibiaxial Flexural Strength of Advanced Ceramics at Ambient Temperature, Annual Book of ASTM Standards, ASTM International, West Conshohocken, Pennsylvania, 2019.
[4] ASTM C769-15(2020), Standard Test Method for Sonic Velocity in Manufactured Carbon and Graphite Materials for Use in Obtaining an Approximate Value of Young's Modulus, Annual Book of ASTM Standards, ASTM International, West Conshohocken, Pennsylvania, 2020.
[5] ASTM D7779-20, Standard Test Method for Determination of Fracture Toughness of Graphite at Ambient Temperature, Annual Book of ASTM Standards, ASTM International, West Conshohocken, Pennsylvania, 2020.

with diameter no less than 0.51 in. (12.95 mm) and length no less than 19/4 in. (120.65 mm);[2] these dimensions are larger than the allowable irradiation capsule volume[6] and oxidation apparatus[7]. Therefore, the ASTM D8289 *Standard Test Method for Tensile Strength Estimate by Disc Compression of Manufactured Graphite*[8] was developed by using the splitting tensile test to provide another way to estimate tensile properties using specimens that have severe geometric constraints and otherwise cannot meet the prescribed testing geometries of ASTM C749. The test method of ASTM D8289 utilizes small disc-shaped specimens with diameters ranging from 6 to 12.7 mm and thicknesses no larger than the corresponding disc radius. The small-specimen geometry in ASTM D8289 is compatible with that of environmental effects specimens, thus allowing for investigation of tensile strength[9] and the effects of various environmental conditions (e.g., irradiation, irradiation creep, molten salt degradation, or oxidation). The measured splitting tensile strength in ASTM D8289 is reported as an estimation of uniaxial counterpart.

2. SMALL-SIZE DISC COMPRESSION TEST STANDARD

The development of small-scale mechanical testing techniques as the alternative of conventional large-scale testing was mainly driven by the need to measure mechanical properties at smaller length scales owing to increasing device miniaturization, as well as the need for microstructure design from the physical point of view.[10] Particularly, the need for testing irradiated materials in a limited volume to minimize the radiation dose directly led to the development of small-specimen test technology and standards.[8,11,12,13]

Instead of using the uniaxial tensile method, the Brazilian disc compression method uses compression load to create tensile stress in the disc. As mentioned in section 1, the ASTM D8289 *Standard Test Method for Tensile Strength Estimate by Disc Compression of Manufactured Graphite*[8] was developed by using the splitting tensile test to provide another way to estimate tensile properties using specimens that have severe geometric constraints and otherwise cannot meet the prescribed testing geometries of ASTM C749. In ASTM D8289 Standard the disc specimens should have diameters ranging from 6 to 12.7 mm and thicknesses no larger than their corresponding radius. Figure 1 shows the test setup of such a small disc compression test. In an ideal situation, a uniform tensile stress will occur at more than half of the disc center line (A–B line as shown in Figure 1b) when the disc is under vertical compression, leading to a center crack caused by the splitting tensile stress at the failure point of the test. Thus the measured tensile stress in the ASTM D8289 Standard could be treated as a good estimation of tensile strength obtained from conventional uniaxial tensile test by following the ASTM C749 Standard. Because of contact friction between the fixture and disc, specific arc geometries are defined in the ASTM D8289 Standard to prevent any early local failure at the two compression ends or big cracks far away from the center line.

---

[6] Burchell TD, McDuffee JL, Thoms KR. Small Specimen data from a high temperature HFIR irradiation experiment. Oak Ridge National Lab. (ORNL), Oak Ridge, TN (United States). High Flux Isotope Reactor (HFIR); 2014 Jan 1.

[7] ASTM D7542-21, Standard Test Method for Air Oxidation of Carbon and Graphite in the Kinetic Regime, Annual Book of ASTM Standards, ASTM International, West Conshohocken, Pennsylvania, 2021.

[8] ASTM D8289-19, Standard Test Method for Tensile Strength Estimate by Disc Comparison of Manufactured Graphite, Annual Book of ASTM Standards, ASTM International, West Conshohocken, Pennsylvania, 2020.

[9] T.D. Burchell, Mersen Grade 2114: A Comparison of Tensile Strength Data, ORNL/TM-2020/1458, Oak Ridge National Laboratory, Oak Ridge, Tennessee, 2020.

[10] Jaya BN, Mathews NG, Mishra AK, Basu S, Jacob K. Non-conventional Small-Scale Mechanical Testing of Materials. Journal of the Indian Institute of Science. 2022 Jan;102(1):139-71.

[11] Klueh RL. Miniature tensile test specimens for fusion reactor irradiation studies. Nuclear engineering and design. Fusion. 1985 Jan 1;2(3):407-16.

[12] Lucas GE, Odette GR, Matsui H, Möslang A, Spätig P, Rensman J, Yamamoto T. The role of small specimen test technology in fusion materials development. Journal of nuclear materials. 2007 Aug 1;367:1549-56.

[13] Bakaev A, Terentyev D, Zinovev A, Chang CC, Yin C, Bakaev VA, Zhurkin EE. Application of sub-miniaturized bending tests to extract tensile properties from neutron-irradiated metallic alloys. Journal of Nuclear Materials. 2022 Jan 1;558:153320.

Geometries of the Ø12.7 mm specimen along with the size of allowable minimum and maximum specimens, are shown in Figure 2. During the development of the ASTM D8289 Standard, an interlaboratory study was conducted to establish a precision statement for D8289. Two different graphite grades (Mersen 2114 and NBG-18) and specimens with two different sizes (Ø6 mm × 3 mm and Ø12.7 mm × 6.35 mm) were tested at seven institutions. Results confirmed that the measured splitting tensile strength from the ASTM D8289 Standard was a good estimation of uniaxial tensile strength for graphites. A comparison between the uniaxial tensile strength tested from the ASTM C749 method and the splitting tensile strength tested from the ASTM D8289 method also supported this conclusion[9] for fine-grain graphite. In the aforementioned disc compression tests,[8,9] the disc thickness was equal to half the disc diameter; no other thicknesses were investigated. The splitting tensile strength in the ASTM D8289 Standard is calculated using Eq. (1), in which P is the peak force before disc failure, L is the disc thickness, and R denotes the disc radius. The coefficient 0.931 acts for the effect of the distributed contact force between fixture and disc while their contact angle is 30°.

$$\sigma_{sts} \approx 0.931 \frac{P}{\pi L R} \tag{1}$$

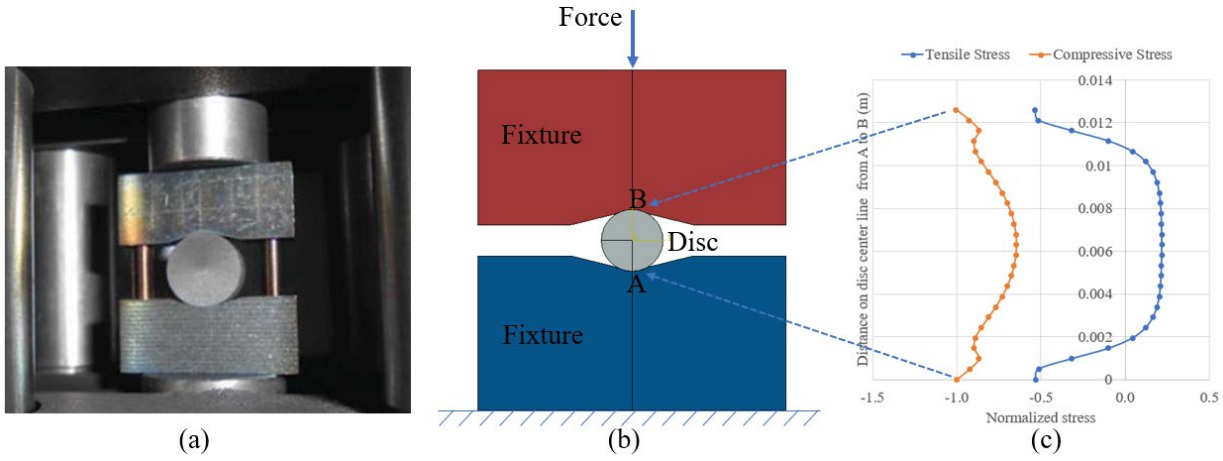

Figure 1. ASTM D8289 disc compression test illustration. (a) Test setup, (b) illustration of load and fixture, (c) ideal normalized stress distribution along center line A–B by taking the absolute compressive stress at point A or B as reference.

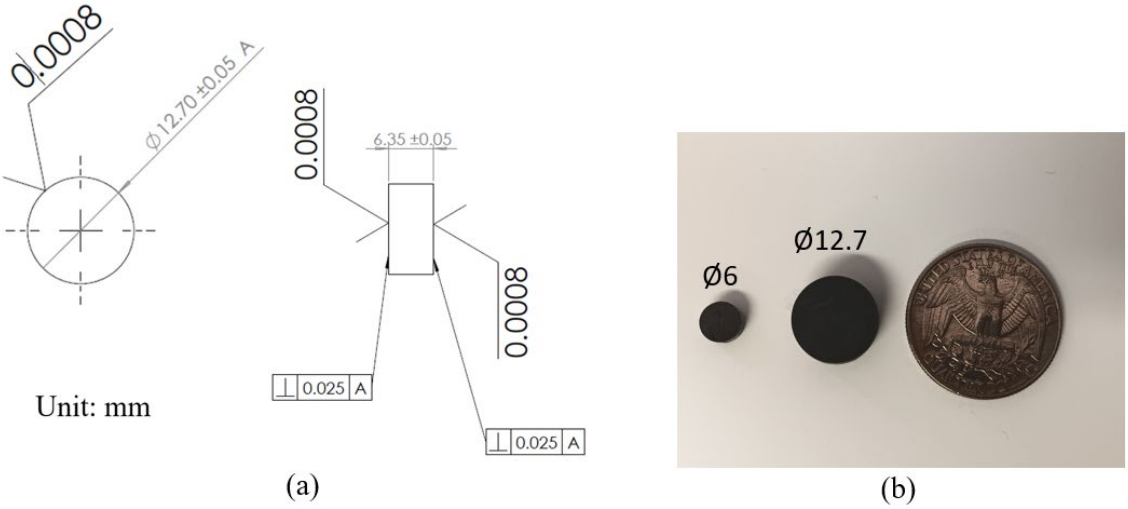

Figure 2. Geometry of graphite disc. (a) Dimensions of Ø12.7 mm sample, (b) size comparison of Ø6 mm, Ø12.7 mm samples.

3. INTEGRATION OF DIC WITH SPLIT DISC TESTING FOR STRAIN CHARACTERIZATION

Although contact extensometers are commonly used in conventional tensile tests, they may not be suitable for disc-splitting tests because the gage section is missing from the specimen itself and because of limitations in correlating the crosshead displacement with nonuniform strain distribution in the specimen. Consequently, noncontact full-field strain measurement techniques are essential for small-size disc-splitting test if the strains can provide more useful information from the test other than the measured splitting tensile strength. Noncontact full-field displacement measurement methods, such as DIC,[14,15,16] digital volume correlation,[17], and electronic speckle pattern interferometry[18] have been developed for scenarios in which traditional point-to-point measurements from extensometers and strain-gauge sensors are inadequate. Among these methods, the DIC technique is more cost-effective, is subject to fewer environment requirements, and is more feasible to deploy than electronic speckle pattern interferometry or digital volume correlation, leading to a huge range of potential applications.[19]

The DIC technique has been used in graphite mechanical tests to observe crack nucleation, initiation, and propagation. As a noncontact full-field method, it works with different specimen geometries and test configurations (e.g., four-point bending,[20] three-point bending with single-edge notched beams,[21] ring-on-ring bending[22]). Because the DIC method can capture abundant information near the crack tip or local stress-concentration region, other important information—including the fracture process zone, J-integral value, and stress intensity factor—can be determined. The full-field displacement/strain measured by DIC can also be integrated using an inverse method to characterize nuclear graphite's mechanical properties, such as Young's modulus and Poisson's ratio.[23] Figure 3 shows the principal idea of image correlation and its calculation of displacement and strains by tracking the pixels in an image subset that is filled with a black-and-white pattern. By finding the maximum of the correlation coefficient (C in Eq. [2]) between the pixels in original subset S and pixels in deformed subset S_1, as shown in Figure 3, the subset deformation can be calculated. The strains of the deformed subset can then be determined by the differentials of the displacement.

[14] J. D. Helm, R. M. Stephen, and M. A. Sutton. Improved three-dimensional image correlation for surface displacement measurement, Opt. Eng. 35, no. 7 (1996): 1911–1920.
[15] M. A. Sutton, J.-J. Orteu, H. W. Schreier, in: Image Correlation for shape motion and deformation measurements: basic concepts, theory and applications. Springer Science & Business Media, New York, 2009.
[16] W.H. Peters, W.F. Ranson, Digital imaging techniques in experimental stress analysis, Opt. Eng. 21, no. 3 (1982) 427–431.
[17] B.K. Bay, T.S. Smith, D.P. Fyhrie, M. Saad, Digital volume correlation: three-dimensional strain mapping using X-ray tomography. Exp. Mech. 39 no. 3 (1999) 217–226.
[18] A.J. Moore, J.R. Tyrer, An electronic speckle pattern interferometer for complete in-plane displacement measurement. Meas. Sci. Technol. 1 no. 10 (1990) 1024.
[19] N. McCormick, J. Lord, Digital Image Correlation, Mater. Today 13 no. 12 (2010) 52–54.
[20] H. Li, J. Duff, T.J. Marrow, In-situ observation of crack nucleation in nuclear graphite by digital image correlation, Proceedings of the ASME Pressure Vessels and Piping Conference 2008 Volume 6: Materials and Fabrication, Parts A and B, Chicago, Illinois, July 27–31, 2008, pp. 813–820.
[21] H. Li, J. Li, G. Singh, A. Fok, Fracture behavior of nuclear graphite NBG-18, Carbon 60 (2013) 46–56.
[22] M. Mostafavi, J. Duff, R. Delorme, T.J. Marrow, Damage nucleation in nuclear graphite under biaxial flexural loading, In: Proceedings of the 9th International Conference on Multiaxial Fatigue and Fracture, Parma, Italy, June 7–9, 2010.
[23] J.D. Lord, N.J. McCormick, J.M. Urquhart, G.M. Klimaytys, I.J. Lingham, Measuring the static modulus of nuclear graphite from four-point flexural strength tests and DIC, Appl. Mech. Mater. 24 (2010) 385–390.

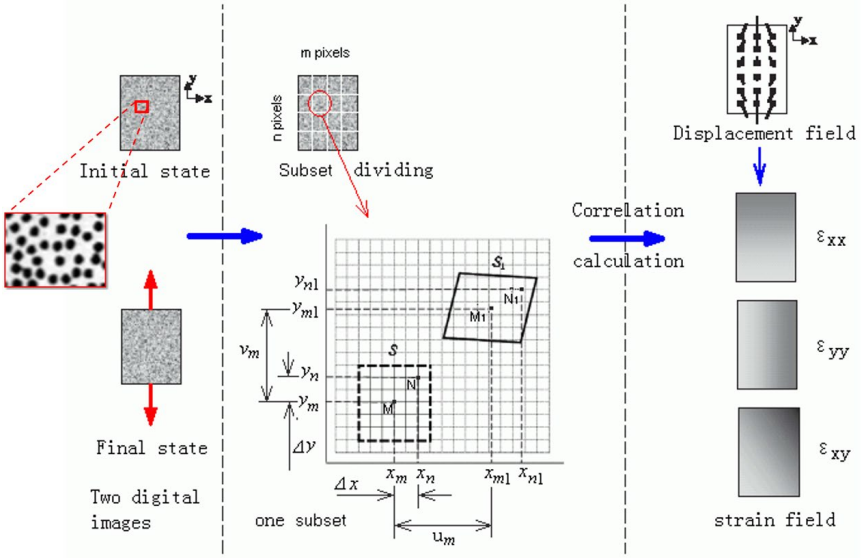

Figure 3. Illustration of the DIC method.

$$C = \frac{\sum_{N \in S}[f(x_n, y_n) - f_d(x_{n1}, y_{n1})]^2}{\sum_{N \in S}[f(x_n, y_n)]^2} \tag{2}$$

$$\begin{cases} x_{n1} = x_m + u_m + \left(1 + \left.\frac{\partial u}{\partial x}\right|_M\right) \cdot \Delta x + \left.\frac{\partial u}{\partial y}\right|_M \cdot \Delta y \\ y_{n1} = y_m + v_m + \left(1 + \left.\frac{\partial v}{\partial y}\right|_M\right) \cdot \Delta y + \left.\frac{\partial v}{\partial x}\right|_M \cdot \Delta x \end{cases} \tag{3}$$

4. EVALUATING THE EFFECT OF SAMPLE THICKNESS ON SPLITTING DISC TESTS

By following the ASTM D8289 Standard, graphite discs with Ø12.7mm but different thicknesses were prepared for the splitting-disc test. This work focused on two fine-grain graphites: Mersen 2114 and IG-110. The test sample matrix is listed in Table 1. Before the test, each disc sample was prepared by spray painting one surface full of homogeneous fine black and white dots; the other surface remained the original black color. For the Mersen 2114 graphite, the samples were labeled from M6S1 to M6S8 for the 6.35 mm thickness discs, M5S1 to M5S8 for the 5 mm thickness discs, M4S1 to M4S8 for the 4 mm thickness discs, and M3S1 to M3S8 for the 3 mm thickness discs. A similar labeling scheme was applied to the IG-110 samples, but the initial letter was changed from M to I.

Table 1. Graphite samples test matrix and properties[24]

Graphite grade	Graphite properties			Sample diameter (mm)	Sample thickness (mm)	Number of samples tested
	Grain size (μm)	Bulk density ($g \cdot cm^{-3}$)	Porosity (%)			
2114	13	1.81	19	12.7	6.35	8
					5	8
					4	8
					3	8
IG-110	10	1.76	21	12.7	6.35	8
					5	8
					4	8
					3	8

Figure 4 shows the ASTM D8289 Standard–compliant disc compression test setup. The Instron 4465 load frame is used to apply the compression load. Its load cell capacity is 5 kN, higher than the peak load required to crack all the disc samples in this test. The loading force is applied via displacement control mode in a rate of 0.2286 mm/min (0.009 in./min), which is slow enough to satisfy the requirement of minimum 30 s rupture time in the ASTM D8289 Standard. The geometry of the fixture also follows the dimensions suggested by the Standard to maintain a 30° contact angle between fixture and disc sample.

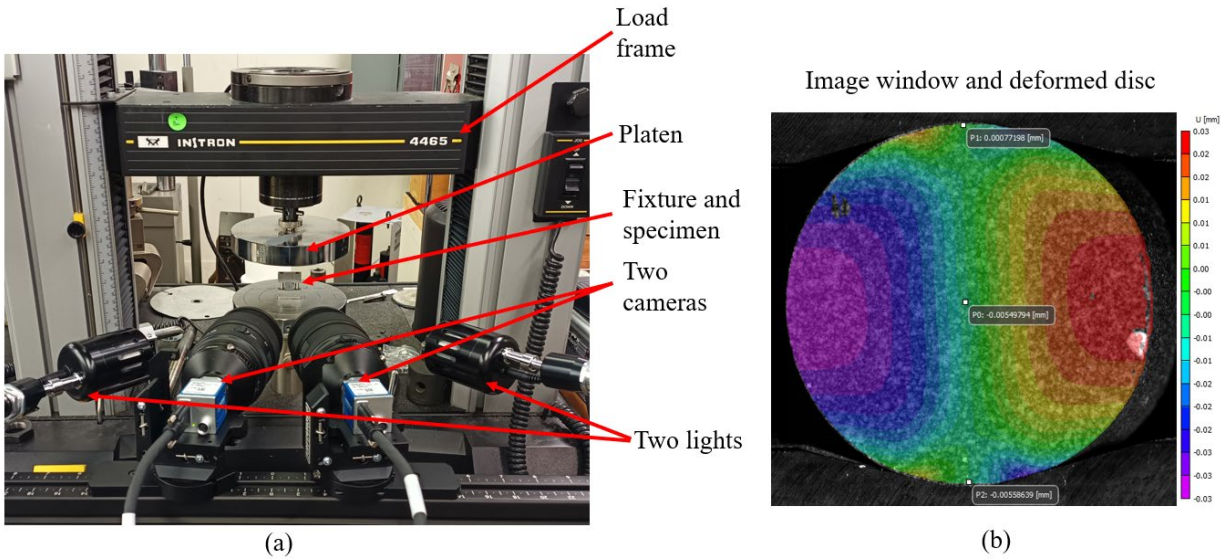

Figure 4. Disc compression test setup.

In addition to the load frame, a DIC system is set up nearby to capture the disc deformation throughout the entire compression procedure until final disc failure. Two Basler 8.0 megapixel digital cameras (2,840 × 2,840 at 40 frames per second) are employed in this DIC system to record both the in-plane and out-of-plane deformations on the painted disc surface. Extra light sources shown in Figure 4a help illuminate the specimen surface, guaranteeing a sufficient aperture, high-contrast disc surface image and

[24] Gallego NC, Contescu CI, Keiser J. Progress report on graphite-salt intrusion studies. Oak Ridge National Lab.(ORNL), Oak Ridge, TN (United States); 2020 Jul 1.

the fast frame rate of 40 frames per second. The angle between two cameras is about 20°. After calibration, the spatial resolution of the recorded image reaches about 203 pixels per millimeter. The effective rectangular image window that has 2,856 × 2,848 pixels includes the entire disc surface and part of the fixture. In general, the disc surface fills about 75% of the 8 megapixel image area, maximumly taking advantage of the effective image pixels for correlation analysis while measuring the full-disc deformations and strains. Figure 4b illustrates the full image window and the effective correlation analysis region that the disc surface occupies. For the image correlation, the subset size is set as 87 pixels, and the analyze step is set as 7.

5. RESULTS

After collecting the peak load from the load-displacement history, the splitting tensile strength of each specimen is listed in Table 2 for Mersen 2114 group and Table 3 for IG-110 group.

Table 2. Test result of Mersen 2114 samples

Sample disc thickness (mm)	Peak load (N)	Splitting tensile strength σ_{sts} (MPa)	Average splitting tensile strength σ_{sts} (MPa)	Deviation of σ_{sts} (MPa)
6.35	3933.18	28.91	28.92	0.79
	4009.53	29.47		
	3939.76	28.95		
	4068.76	29.90		
	3931.86	28.90		
	4033.22	29.64		
	3798.91	27.92		
	3763.37	27.66		
5	3132.85	29.24	29.87	0.64
	3159.18	29.49		
	3163.13	29.52		
	3275.02	30.57		
	3182.87	29.71		
	3171.03	29.60		
	3184.19	29.72		
	3335.57	31.13		
4	2499.70	29.16	29.48	0.60
	2532.61	29.55		
	2564.20	29.92		
	2516.81	29.36		
	2474.69	28.87		
	2631.33	30.70		
	2479.96	28.93		
	2512.86	29.32		
3	1957.38	30.45	29.81	0.59
	1909.99	29.71		
	1942.90	30.22		
	1832.32	28.50		
	1933.68	30.08		
	1930.39	30.03		
	1915.91	29.80		
	1909.99	29.71		

Table 3. Test results of IG-110 samples

Sample disc thickness (mm)	Peak load (N)	Splitting tensile strength σ_{sts} (MPa)	Average splitting tensile strength σ_{sts} (MPa)	Deviation σ_{sts} (MPa)
6.35	3002.54	22.07	21.80	0.68
	2931.46	21.54		
	3110.48	22.86		
	2918.29	21.45		
	3070.99	22.57		
	2935.40	21.57		
	2820.88	20.73		
	2936.72	21.58		
5	2377.28	22.19	22.03	0.54
	2378.60	22.20		
	2400.98	22.41		
	2302.25	21.49		
	2432.57	22.70		
	2252.23	21.02		
	2350.96	21.94		
	2385.18	22.26		
4	1911.30	22.30	22.12	0.78
	1929.73	22.51		
	1908.67	22.27		
	1930.39	22.52		
	1941.58	22.65		
	1734.26	20.23		
	1897.48	22.14		
	1912.62	22.31		
3	1488.11	23.15	21.58	1.55
	1286.71	20.02		
	1467.04	22.82		
	1441.38	22.42		
	1424.26	22.16		
	1199.83	18.66		
	1432.82	22.29		
	1355.81	21.09		

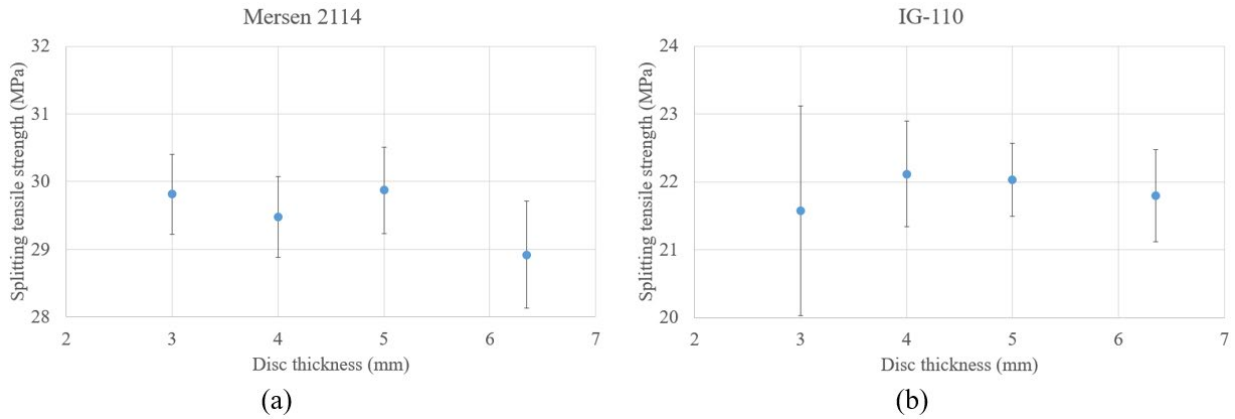

(a) (b)

Figure 5. Relation between disc thickness and splitting tensile strength.

As shown in Figure 5, both fine-grain graphites exhibit a slight increase of splitting tensile strength when the disc thickness decreases from the maximum allowed value (6.35 mm). On average, the splitting tensile strengths of Mersen 2114 samples in 3 mm thick, 4 mm thick, and 5 mm thick discs are close to each other, but all higher than the 28.92 MPa value obtained from the 6.35 mm thickness samples. For the IG-110 samples, the 3 mm thickness discs have an exceptional average splitting tensile strength of 21.58 MPa, lower than its 6.35 mm thickness discs (21.80 MPa). However, the average splitting tensile strengths of 4 mm and 5 mm thick discs are higher than those of the 6.35 mm discs. The higher porosity and larger pores in IG-110 than Mersen 2114 might contribute to the relative lower strength of the IG-110 3 mm thickness discs. When the specimen thickness decreases, the weak pores are more likely to be exposed in the thickness direction; therefore, they affect the failure load more significantly. The much larger strength standard deviation of the IG-110 discs with 3 mm thickness than the others strongly indicate that result as well.

The Mersen 2114 and IG-110 graphites have been tested comprehensively to characterize their mechanical properties, including the tensile strength obtained from traditional uniaxial tensile test by following the ASTM C749 Standard. A total of 45 Mersen 2114 specimens[25] have been tested according to the ASTM C749 method, obtaining an average tensile strength of 28.89 MPa with a standard deviation of 4.29 MPa. Different uniaxial tensile test results of IG-110 can be found in the literature,[26] such as 29.6 ± 5.9 MPa obtained from averaging 640 samples,[27], or 24.4 ± 2.9 MPa obtained from averaging 80 samples.[28] Figure 6 compares the tensile strength between the splitting-disc method results in the present work and results of the uniaxial tensile test method in the literature. Although small variances are shown in the Mersen 2114 samples with different thicknesses, their averaged splitting tensile strengths, 28.92 MPa for 6.35 mm thickness, 29.87 MPa for 5 mm thickness, 29.48 MPa for 4 mm thickness, and 29.81 MPa for 3 mm thickness agree well with the reference value 28.89 MPa obtained from 45 uniaxial tensile test samples. However, the averaged splitting tensile strengths of IG-110 samples with different disc thicknesses in the current study (about 22.0 MPa) are all lower than the referenced uniaxial tensile strengths (29.6 or 24.4 MPa[27,28]).

[25] T. D. Burchell, Mersen Grade 2114: Tensile Strength from Brazilian Disc Testing, ORNL/TM-2020/1485, March 2020.
[26] M. Srinivasan, B. Marsden, W. von Lensa, L. Cronise, R. Turk, Appendices to the Assessment of Graphite Properties and Degradation, Including Source Dependence, TLR/RES/DE/REB-2021-08, Aug 2021.
[27] Sumita J, Shibata T, Iyoku T, Sawa K, Hanawa S, Ishihara M. Characteristics of first loaded ig-110 graphite in httr core. Japan Atomic Energy Agency; 2006.
[28] Ishihara M, Mogi H, Ioka I, Arai T, Oku T. Statistical considerations of graphite strength for assessing design allowable stresses. 1987.

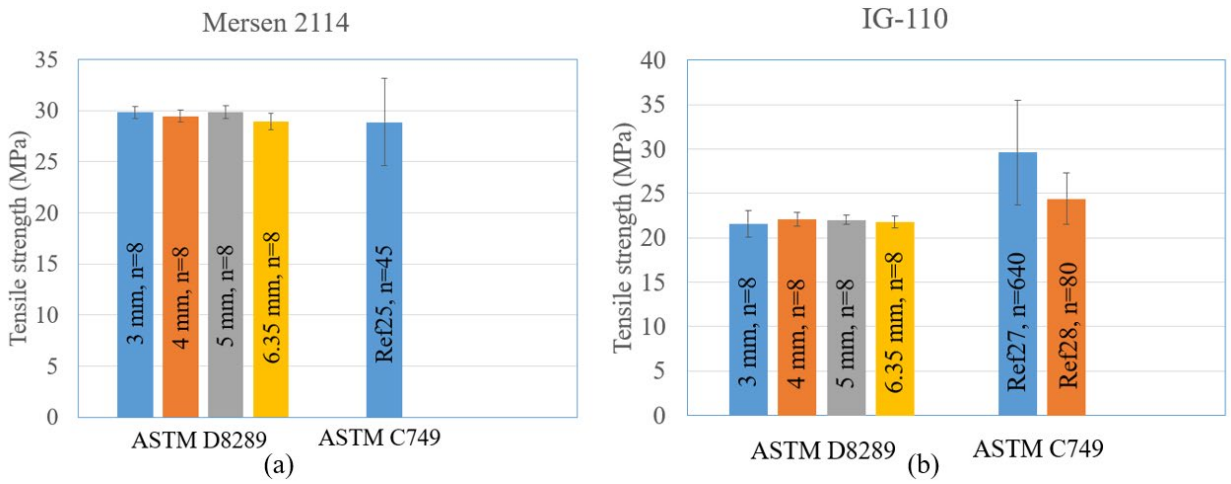

Figure 6. Comparison between splitting tensile strength and uniaxial tensile strength. (a) Mersen 2114 and (b) IG-110.

In addition to the splitting tensile strength, the high-resolution DIC images recorded the full-field displacement and strains on the disc surface that was painted with black and white dots. Taking the Mersen 2114 6.35 mm thick sample M6S4 and the IG-110 6.35 mm thick sample I6S2 as examples, Figure 7 and Figure 8 show plots of the displacement fields and strain fields on the disc surface at the moment of peak load (last frame before crack). The DIC results clearly show the high tensile strain (e_{xx}) at the disc center region; this strain led to the splitting crack in that high-stress area owing to graphite's weaker tensile strength than compressive strength. Strong shear strains (e_{xy}) were observed at the four contact corners in Figure 7f and Figure 8f. The two-camera setup in the DIC system allowed for the image correlation analysis to detect significant out-of-plane displacements (W) on the compressed disc throughout the central region from top to bottom, particularly at the disc top in contact with the fixture.

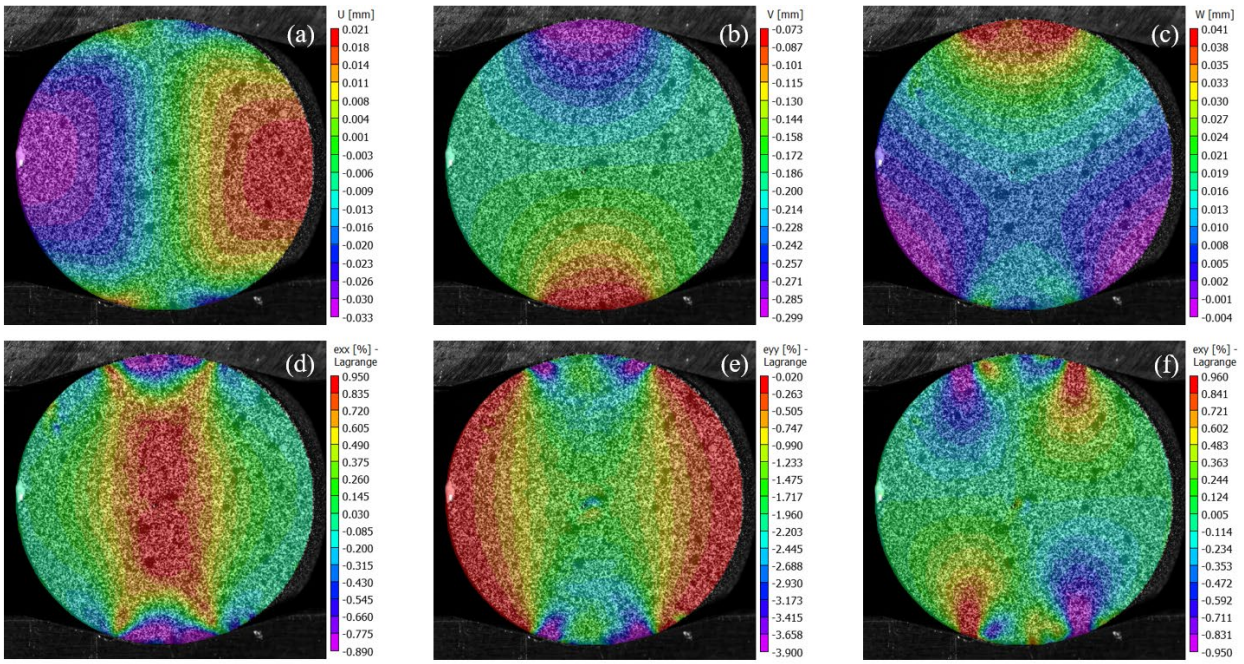

Figure 7. Displacement and strain fields of Mersen 2114 6.35mm thick sample M6S4 before failure.
(a) Horizontal displacement U, (b) vertical displacement V, (c) out-of-plane displacement W, (d) horizontal strain e_{xx}, (e) vertical strain e_{yy} and (f) shear strain e_{xy}.

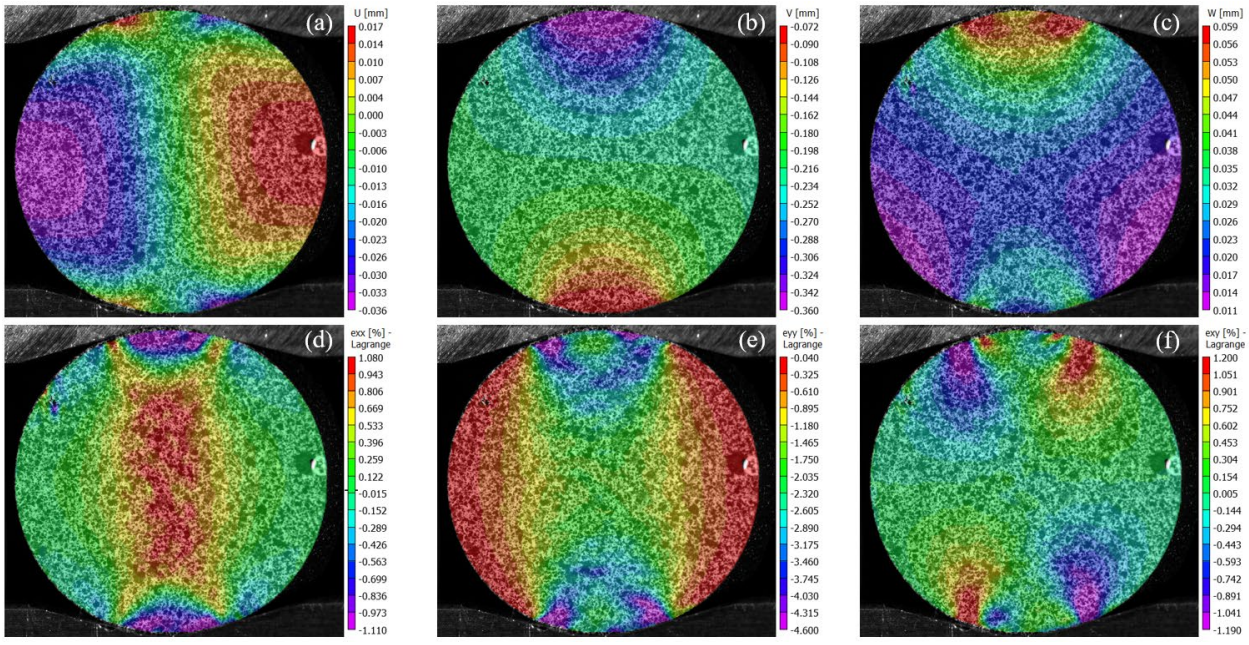

Figure 8. Displacement and strain fields of IG-110 6.3mm thick sample I6S2 before failure. (a) Horizontal displacement, (b) vertical displacement, (c) out-of-plane displacement, (d) horizontal strain, (e) vertical strain, and (f) shear strain.

The displacement and strain development of these two representative samples throughout the loading history are illustrated in Figure 9. As shown in Figure 9a and Figure 9c, the out-of-plane displacement (~0.01–0.02 mm) at disc center before failure is about one order of magnitude smaller than the vertical

displacement (~0.2 mm). Meanwhile, the horizontal strain (tensile) and vertical strain (compressive) in Figure 9b and Figure 9d show a slight nonlinearity, particularly after 100 s.

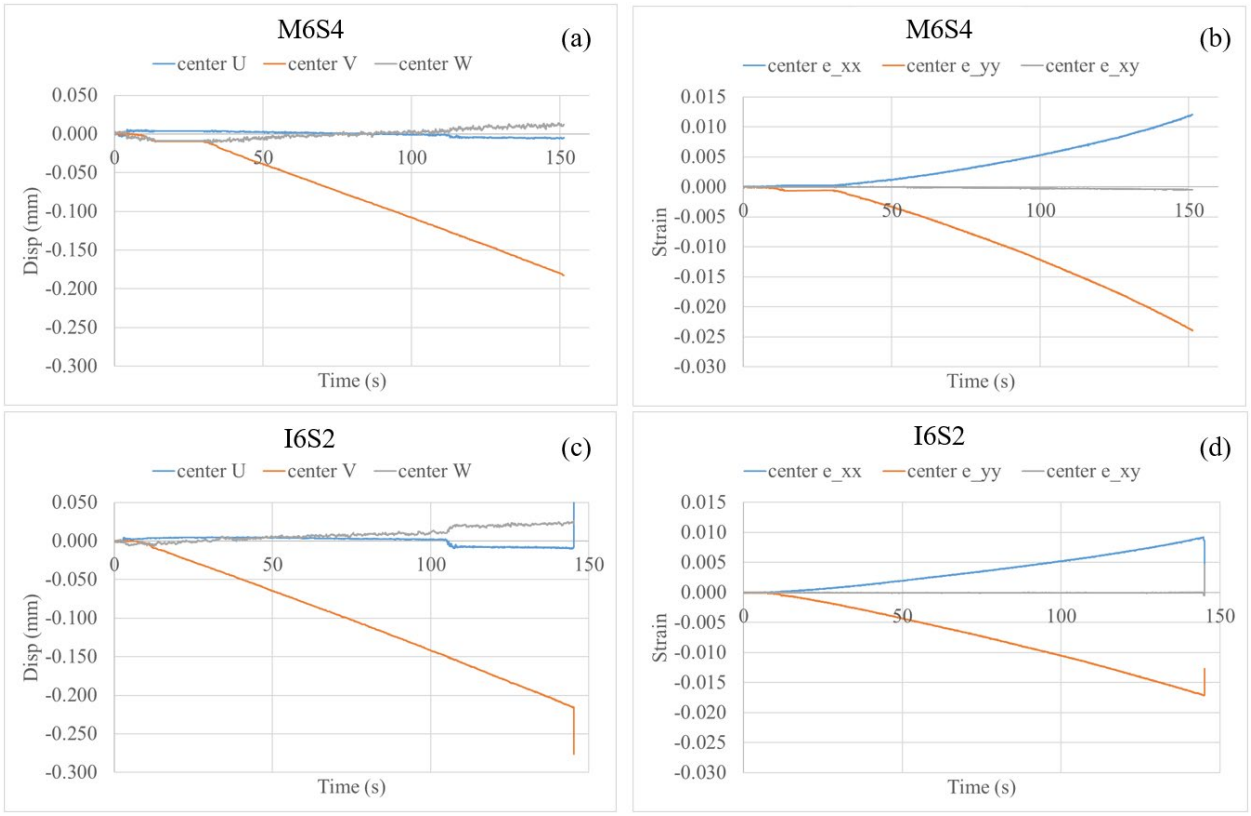

Figure 9. Displacement and strain development of samples M6S4 and I6S2 at disc center. (a) M6S4 displacement history, (b) M6S4 strain history, (c) I6S2 displacement history, and (d) I6S2 strain history.

Figure 10 shows a significant out-of-plane displacement (~0.05 mm), which was observed on both M6S4 and I6S2 specimens near the top region in contact with the fixture before the disc failed. The same out-of-plane displacement at disc center or disc bottom was smaller than at the top location but was still detectable with the high-resolution DIC system. The peak load on M6S4 (4,068.76 N) was higher than the I6S2 (2,931.46 N) specimen; however, more vertical displacement (V) and out-of-plane displacement (W) were observed on the I6S2 specimen than on the M6S4 specimen at center, top, and bottom locations. The load and displacement/strain measurements indicate IG-110's weaker splitting tensile strength compared with Mersen 2114. They also indicate more local nonlinear behavior, such as the strains shown in Figure 11b, or nonplane-stress behavior of the IG-110 specimen. When the specimen thickness is reduced from 6.35 to 3 mm, these local nonlinear behaviors may lead to more early-stage fracture at two loading ends, therefore significantly affecting the final splitting tensile strength. For the other 2114 and IG-110 specimens in this study, the measured DIC results at the same location varied with the peak load and thickness accordingly, but their full-field distribution on the disc was similar to specimens M6S4 and I6S2.

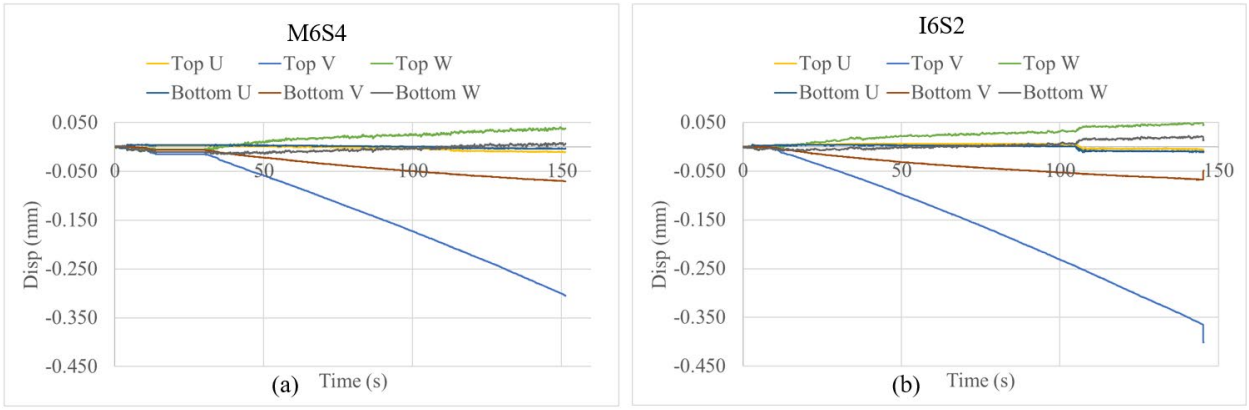

Figure 10. Displacement history on the disc top and bottom. (a) Specimen M6S4, (b) specimen I6S2.

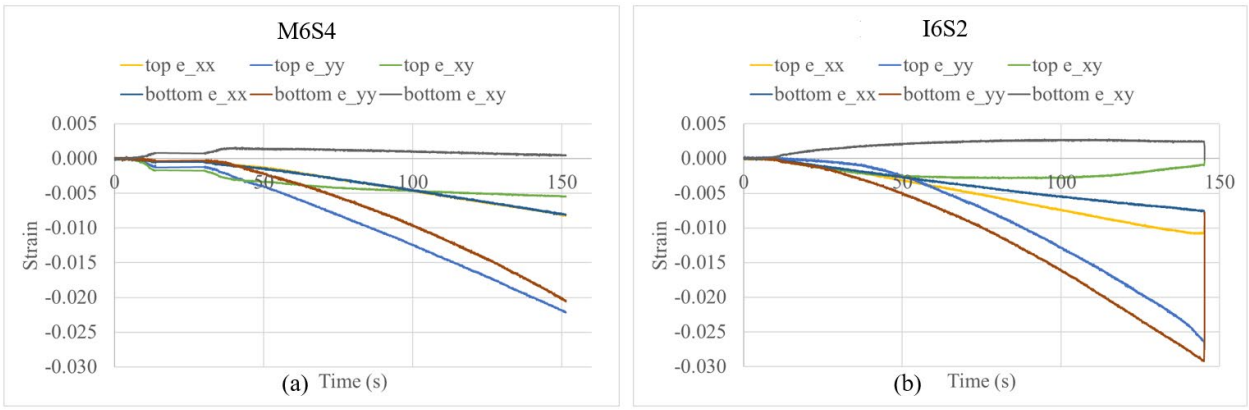

Figure 11. Strain history on the disc top and bottom. (a) Specimen M6S4, (b) specimen I6S2.

6. CONCLUSIONS

This work investigated the correlation between disc thickness and disc splitting tensile strength of two fine-grain graphites, Mersen 2114 and IG-110. By following the ASTM D8289 test standard, eight samples of each thickness group were compressed to failure to obtain their splitting tensile strengths. Results showed the tendency of a small increase in splitting tensile strength when the disc thickness decreased in both Mersen 2114 and IG-110 samples. The 3 mm thick IG-110 samples showed a reverse trend and a larger standard deviation in splitting tensile strength, indicating that these discs were too thin to obtain a stable experiment result compared with the other thicknesses. The Mersen 2114 samples in the same thickness did not have this problem. Meanwhile, the splitting tensile strengths of Mersen 2114 samples in this study agreed with uniaxial tensile strength tested from ASTM C749. The IG-110 samples in different thicknesses had lower splitting tensile strengths than the referenced uniaxial tensile test values. The DIC results confirmed the high tensile strain region around the disc center that eventually led to the major vertical center crack. Significant out-of-plane displacement and nonlinearity were measured at disc top and bottom compared with the disc center. Splitting tensile strength and DIC results both indicated that IG-110 is a softer material than Mersen 2114.